Journal of Sound and Vibration (2002) **258**(1), 147–165
doi:10.1006/jsvi.5107, available online at http://www.idealibrary.com on IDEAL®

ANALYSES OF DYNAMIC RESPONSE OF VEHICLE AND TRACK COUPLING SYSTEM WITH RANDOM IRREGULARITY OF TRACK VERTICAL PROFILE

X. Lei

Department of Civil Engineering, East China Jiaotong University, Nanchang 330013, *People's Republic of China. E-mails: xiaoyanlei@yahoo.com.cn, leixy@ecjtu.jx.cn*

AND

N.-A. Noda

Department of Mechanical Engineering, Kyushu Institute of Technology, 804-8550, Japan

(*Received* 6 *April* 2001, *and in final form* 4 *March* 2002)

A dynamic computational model for the vehicle and track coupling system is developed by means of finite element method in this paper. In numerical implementation, the vehicle and track coupling system is divided into two parts; lower structure and upper structure. The vehicle as the upper structure in the coupling system is a whole locomotive or rolling stock with two layers of spring and damping system in which vertical and rolling motion for vehicle and bogie are involved. The lower structure in the coupling system is a railway track where rails are considered as beams with finite length rested on a double layer continuous elastic foundation. The two parts are solved independently with an iterative scheme. Coupling the vehicle system and railway track is realized through interaction forces between the wheels and the rail, where the irregularity of the track vertical profile considered as stationary ergodic Gaussian random processes and simulated by trigonometry series is included. The amplitudes of vibrations, their velocities and the accelerations generated in the vehicle and rail and the interaction forces between the vehicle and the rail due to the random irregularity of the track vertical profile and different line grades and train speeds have been analyzed numerically by this model. Analyses of system responses are performed in time and frequency domains.

© 2002 Elsevier Science Ltd. All rights reserved.

1. INTRODUCTION

It is well known that profile irregularity of the railway line is one of the essential vibration sources to vehicle and track. It is a dominating source for rolling noise too. With the increase of train speed, axle load and volume of traffic, the vibration of the vehicle and track coupling system will be intensified, the safe operation of trains will be reduced and the dynamic forces acting on the track structure will be increased significantly. As a result, fatigue and damage of components of the track structure will emerge, and settlement of the rail will occur under repeated action of dynamic loads. The deterioration of the railway conversely intensifies the vibration of locomotives and rolling stocks. Eventually, the operation quality of trains will be lowered and the service life of rails will be reduced. Hence, in order to alleviate the forces acting on the rails, prolong its service life

0022-460X/02/$35.00 © 2002 Elsevier Science Ltd. All rights reserved.

and ensure the safe operation of trains, it is necessary to comprehensively study dynamic responses of the vehicle and track coupling system with random irregularity of the railway line.

Some studies [1–14] have focused on the vibration in a railway track under moving vehicles, and different theories and models have been presented. Early studies referred to two typical theories [1–5]: continuous support model and discrete support model. These models are simple, but are inadequate in understanding vibration characteristics of the vehicle and track system since the coupling behavior between the vehicle and the track is not considered. Later, other detailed models [7–13] were developed, in which the coupling of vehicles and railway track is considered. However, only a few studies [14] have concentrated on analyses of dynamic responses of the vehicle and track coupling system with random irregularity of track profile. In the present paper, a dynamic computational model for the vehicle and track coupling system is formulated by means of finite element method. Also the track vertical profile irregularity is considered as stationary ergodic Gaussian random processes and is included in this model. Analyses of dynamic responses for the coupling system are performed in time and frequency domains. The amplitudes of vibrations, their velocities and the accelerations generated in the vehicle and rail and the interaction forces between the vehicle and the rail due to the random irregularity of the track vertical profile and different train speeds have been obtained and compared with other analyses. Finally, conclusions are given.

2. MODEL FOR VEHICLE AND TRACK COUPLING SYSTEM

2.1. FUNDAMENTAL ASSUMPTIONS

The following assumptions are made in establishing a dynamic computational model of the vehicle and track coupling system.

(1) Only vertical and longitudinal dynamic loads are considered in the model.
(2) The upper structure in the coupling system is a whole locomotive or rolling stock with two layers of spring and damping system in which vertical and rolling motion for vehicle and bogie are involved.
(3) The lower structure in the coupling system is a railway track where rails are considered as beams with finite length resting on a double layer of continuous elastic foundation. (Computation experience shows that as long as the vehicle is 20 m away from the rail ends, the effect of the boundary can be neglected.) The elastic and damping behaviors for rail fastenings and ballast are represented by equivalent stiffness coefficients K_{x1}, K_{y1} and damping coefficients C_{x1}, $C_{y1}$where K_{x1}, C_{x1} and K_{y1}, C_{y1} are stiffness and damping coefficients along the x and y directions respectively.
(4) Masses of ties are treated as centralized masses acting on nodes of beam elements.
(5) Masses of ballast are simplified as centralized masses too and only vertical dynamic responses are considered. The elastic and damping behaviors for roadbed are K_{y2} and C_{y2}.
(6) The conventional Hertz formula for two elastic contact cylinders perpendicular to each other is used in coupling vehicles and railway track.
(7) Since the vehicle and railway track are symmetrical about the centerline of the track, only half of the coupling system is used for the ease of calculation.
(8) The track vertical profile irregularity is considered as stationary ergodic Gaussian random processes which can be obtained by numerical simulation.

The model for the analyses of dynamic responses of the vehicle and track coupling system with random irregularity of the railway line is shown in Figure 1.

2.2. DYNAMIC EQUATION OF VEHICLE

Structure over sprung mass of the locomotive or the rolling stock is considered as a rigid body with some mass. Vertical and rolling motion for vehicle and bogie are considered here. In this case, structure over the track has ten degrees of freedom, i.e., six vertical displacements and three rolling motions.

Defining a whole vehicle as a computational element, the nodal displacement vector and load vector for this element can be expressed as

$$\{a\}_u = \{\, v_c \quad \varphi_c \quad v_{t1} \quad \varphi_{t1} \quad v_{t2} \quad \varphi_{t2} \quad v_{w1} \quad v_{w2} \quad v_{w3} \quad v_{w4} \,\}^T, \tag{1}$$

$$\{Q\}_u = \{\, -M_c g \quad 0 \quad -M_t g \quad 0 \quad -M_t g \quad 0 \quad P_1 \quad P_2 \quad P_3 \quad P_4 \,\}^{\mathrm{T}}, \tag{2}$$

where $P_i = -M_{wi}g + F_{wi}$, $M_{w1} = M_{w2} = M_{w3} = M_{w4}$, v_c and φ_c are vertical displacement and rolling motion for the rigid body of the vehicle, v_{ti} and φ_{ti} are vertical displacement and the rolling motion for the ith bogie, M_{wi} is the mass of the ith wheel and F_{wi} is the interaction force resulting from the ith wheel of the vehicle contact with the rail.

The dynamic equation of vehicle in the coupling system can be described as

$$[M]_u\{\ddot{a}\}_u + [C]_u\{\dot{a}\}_u + [K]_u\{a\}_u = \{Q\}_u, \tag{3}$$

where $[M]_u$, $[C]_u$ and $[K]_u$ are mass, damping and stiffness matrixes for the upper structure. They are

$$[M]_u = diag\{\, M_c \quad J_c \quad M_t \quad J_t \quad M_t \quad J_t \quad M_{w1} \quad M_{w2} \quad M_{w3} \quad M_{w\,4} \,\}, \tag{4}$$

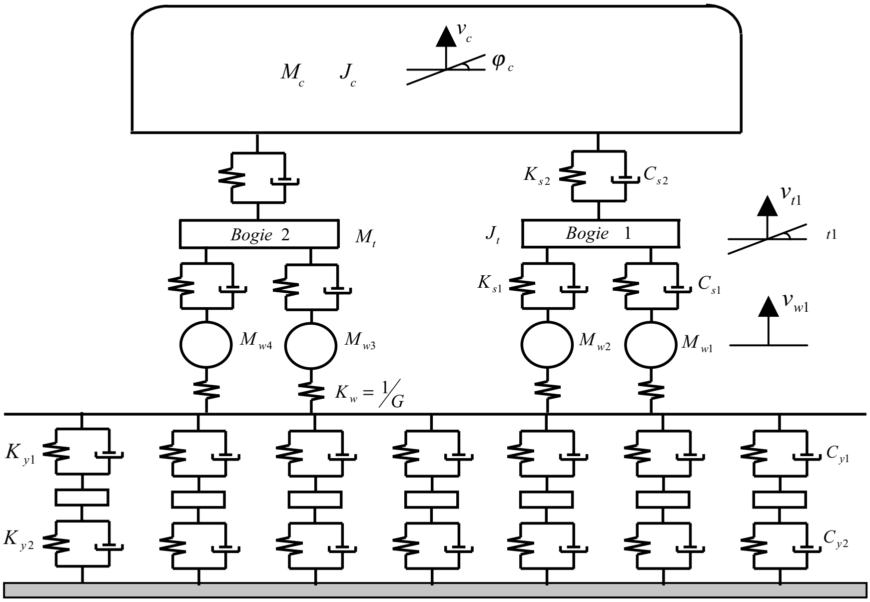

Figure 1. Model for analysis of vehicle and track coupling system.

$$[K]_u = \begin{bmatrix} 2K_{s2} & 0 & -K_{s2} & 0 & -K_{s2} & 0 & 0 & 0 & 0 & 0 \\ & 2L_2^2K_{s2} & -L_2K_{s2} & 0 & L_2K_{s2} & 0 & 0 & 0 & 0 & 0 \\ & & 2K_{s1}+K_{s2} & 0 & 0 & 0 & -K_{s1} & -K_{s1} & 0 & 0 \\ & & & 2L_1^2K_{s1} & 0 & 0 & -K_{s1}L_1 & K_{s1}L_1 & 0 & 0 \\ & & & & 2K_{s1}+K_{s2} & 0 & 0 & 0 & -K_{s1} & -K_{s1} \\ & & & & & 2L_1^2K_{s1} & 0 & 0 & -K_{s1}L_1 & K_{s1}L_1 \\ & & Symm & & & & K_{s1} & 0 & 0 & 0 \\ & & & & & & & K_{s1} & 0 & 0 \\ & & & & & & & & K_{s1} & 0 \\ & & & & & & & & & K_{s1} \end{bmatrix}, \tag{5}$$

$$[C]_u = \begin{bmatrix} 2C_{s2} & 0 & -C_{s2} & 0 & -C_{s2} & 0 & 0 & 0 & 0 & 0 \\ & 2L_2^2C_{s2} & -L_2C_{s2} & 0 & L_2C_{s2} & 0 & 0 & 0 & 0 & 0 \\ & & 2C_{s1}+C_{s2} & 0 & 0 & 0 & -C_{s1} & -C_{s1} & 0 & 0 \\ & & & 2L_1^2C_{s1} & 0 & 0 & -C_{s1}L_1 & C_{s1}L_1 & 0 & 0 \\ & & & & 2C_{s1}+C_{s2} & 0 & 0 & 0 & -C_{s1} & -C_{s1} \\ & & & & & 2L_1^2C_{s1} & 0 & 0 & -C_{s1}L_1 & C_{s1}L_1 \\ & Symm & & & & & C_{s1} & 0 & 0 & 0 \\ & & & & & & & C_{s1} & 0 & 0 \\ & & & & & & & & C_{s1} & 0 \\ & & & & & & & & & C_{s1} \end{bmatrix}. \tag{6}$$

In equations (4)–(6), M_c and J_c are mass and rolling moment of inertia for the rigid body of the vehicle, M_t and J_t are mass and rolling moment of inertia for bogies, $2L_1$ is the distance between the central line of the sprung masses of the two bogies and $2L_2$ is the distance between the central line of two bogies of the same vehicle.

2.3. DYNAMIC EQUATION OF RAILWAY TRACK

Finite element method is employed to establish the dynamic equation of a railway track, where rails as beams with finite length are discretized as two-dimensional (2-D)beam elements and the rail between two neighbor ties is treated as one element. Masses of ties as centralized masses are attached to nodes of beam elements. In order to reduce the bandwidth of the global stiffness matrix of the finite element equation and make programming easy, a generalized beam element [15] for track structure is used here. In the generalized beam element, additional vertical displacement v_i^* for ballast is added to the normal 2-D beam element, i.e. an element with three variables $(u_i,\ v_i,\ \theta_i)$ of each node is changed to one with four variables $(u_i,\ v_i,\ \theta_i,\ v_i^*)$ per node, as shown in Figure 2. The elastic and damping behavior for rail fastenings and ballast as well as roadbed are

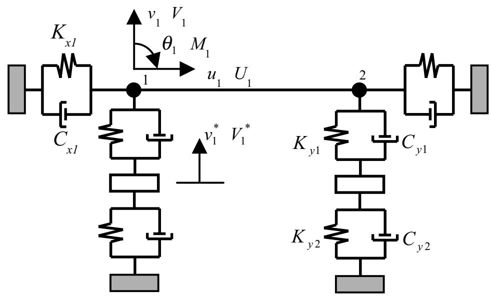

Figure 2. Generalized beam element for track structure.

represented with equivalent stiffness coefficients K_{x1}, K_{y1}, K_{y2} and damping coefficients C_{x1}, C_{y1}, C_{y2}. Hence, we can define nodal displacement vector and nodal force vector for this generalized beam element as follows:

$$\{a\}_l^e = \{\, u_1 \quad v_1 \quad \theta_1 \quad v_1^* \quad u_2 \quad v_2 \quad \theta_2 \quad v_2^* \,\}^{\mathrm{T}}, \tag{7}$$

$$\{F\}_l^e = \{\, U_1 \quad V_1 \quad M_1 \quad V_1^* \quad U_2 \quad V_2 \quad M_2 \quad V_2^* \,\}^{\mathrm{T}}. \tag{8}$$

The stiffness matrix of the element can be expressed as

$$[K]_l^e = [K]_b^e + [K]_e^e = \begin{bmatrix} \frac{EA}{l} & 0 & 0 & 0 & -\frac{EA}{l} & 0 & 0 & 0 \\ & \frac{12EI}{l^3} & -\frac{6EI}{l^2} & 0 & 0 & -\frac{12EI}{l^3} & -\frac{6EI}{l^2} & 0 \\ & & \frac{4EI}{l} & 0 & 0 & \frac{6EI}{l^2} & \frac{2EI}{l} & 0 \\ & & & 0 & 0 & 0 & 0 & 0 \\ & & & & \frac{EA}{l} & 0 & 0 & 0 \\ & Symm & & & & \frac{12EI}{l^3} & \frac{6EI}{l^2} & 0 \\ & & & & & & \frac{4EI}{l} & 0 \\ & & & & & & & 0 \end{bmatrix}$$

$$+ \begin{bmatrix} K_{x1} & 0 & 0 & 0 & 0 & 0 & 0 & 0 \\ & K_{y1} & 0 & -K_{y1} & 0 & 0 & 0 & 0 \\ & & 0 & 0 & 0 & 0 & 0 & 0 \\ & & & K_{y1}+K_{y2} & 0 & 0 & 0 & 0 \\ & & & & K_{x1} & 0 & 0 & 0 \\ & & & & & K_{y1} & 0 & -K_{y1} \\ & Symm & & & & & 0 & 0 \\ & & & & & & & K_{y1}+K_{y2} \end{bmatrix}, \tag{9}$$

where $[K]_b^e$ and $[K]_e^e$ are stiffness matrixes resulting from beam element and elastic supports. E, A and I are modules of elasticity, cross-sectional area and moment of inertia for the rail and l is the length of the element.

The mass matrix of the element is

$$[M]_l^e = [M]_b^e + [M]_e^e = \frac{\rho A l}{420}\begin{bmatrix} 140 & 0 & 0 & 0 & 70 & 0 & 0 & 0 \\ & 156 & -22l & 0 & 0 & 54 & 13l & 0 \\ & & 4l^2 & 0 & 0 & -13l & -3l^2 & 0 \\ & & & 0 & 0 & 0 & 0 & 0 \\ & & & & 140 & 0 & 0 & 0 \\ & Symm & & & & 156 & 22l & 0 \\ & & & & & & 4l^2 & 0 \\ & & & & & & & 0 \end{bmatrix}$$

$$+\begin{bmatrix} m_p & & & & & & & 0 \\ & m_p & & & & & & \\ & & 0 & & & & & \\ & & & m_b & & & & \\ & & & & m_p & & & \\ & & & & & m_p & & \\ & & & & & & 0 & \\ 0 & & & & & & & m_b \end{bmatrix}, \tag{10}$$

where $[M]_b^e$ and $[M]_e^e$ are mass matrixes resulting from beam element and sleeper and ballast. ρ is the density of the rail, m_p and m_b are half masses of the tie and the ballast between two ties respectively.

The damping matrix of the element is usually expressed as

$$[C]_l^e = [C]_b^e + [C]_e^e = \alpha[M]_b^e + \beta[K]_b^e + [C]_e^e, \tag{11}$$

where

$$[C]_e^e = \begin{bmatrix} C_{x1} & 0 & 0 & 0 & 0 & 0 & 0 & 0 \\ & C_{y1} & 0 & -C_{y1} & 0 & 0 & 0 & 0 \\ & & 0 & 0 & 0 & 0 & 0 & 0 \\ & & & C_{y1}+C_{y2} & 0 & 0 & 0 & 0 \\ & & & & C_{x1} & 0 & 0 & 0 \\ & & & & & C_{y1} & 0 & -C_{y1} \\ & Symm & & & & & 0 & 0 \\ & & & & & & & C_{y1}+C_{y2} \end{bmatrix}, \tag{12}$$

where $[C]_b^e$ and $[C]_e^e$ are damping matrixes resulting from beam element and damping components. α and β are damping coefficients which depend upon the damping ratio and the natural frequency of the system. Such a damping is called proportional damping or vibration damping.

The finite element dynamic equation for railway track can be written as

$$[M]_l\{\ddot{a}\}_l + [C]_l\{\dot{a}\}_l + [K]_l\{a\}_l = \{Q\}_l, \tag{13}$$

where

$$[M]_l = \sum_e [M]_l^e, \quad [C]_l = \sum_e [C]_l^e, \quad [K]_l = \sum_e [K]_l^e, \quad \{Q\}_l = \sum_e \{F\}_l^e. \tag{14}$$

These are global mass, damping and stiffness matrixes for lower structure, which can be assembled by matrixes of element mass, element damping and element stiffness.

3. NUMERICAL SIMULATION OF THE RANDOM IRREGULARITY OF TRACK VERTICAL PROFILE

Generally, the irregularity of the track vertical profile can be regarded as stationary ergodic Gaussian random processes except the area with turnout, road crossing and the rail line with track deterioration [16].

Consider a stationary stochastic process $\eta(t)$ with expectation zero and power spectral density function $S_x(\omega)$. The sample function of the stochastic process $\eta(t)$ can be simulated by trigonometry series as [17]

$$\eta^d(t) = \sum_{k=1}^{N} a_k \sin(\omega_k t + \phi_k), \tag{15}$$

where a_k is a Gaussian random variable with expectation zero and variance σ_k and is independent for $k = 1, 2, \ldots, N$, ϕ_k is a random variable with uniformity distribution in $0{-}2\pi$ and is independent for $k = 1, 2, \ldots, N$ too. a_k and ϕ_k are independent of each other and can be generated by computer by multiplicative method, Monte Carlo method or another algorithm of generating pseudo-random variable [18].

In order to obtain variance σ_k, we define a frequency band $\Delta\omega$ as

$$\Delta\omega = (\omega_u - \omega_l)/N, \tag{16}$$

where ω_l and ω_u are the lower and upper limit frequencies in the frequency domain of power spectral density function and N is a sufficient large division number.

Defining

$$\omega_k = \omega_l + (k - \tfrac{1}{2})\Delta\omega, \quad k = 1, 2, \ldots, N, \tag{17}$$

we have

$$\sigma_k^2 = 4S_x(\omega_k)\Delta\omega, \quad k = 1, 2, \ldots, N. \tag{18}$$

In the above computation, the effective power spectral density $S_x(\omega_k)$ is assumed to be in the range of ω_l to ω_u and beyond this scope $S_x(\omega_k)$ is taken as zero.

The power spectral density $S_x(\omega)$ of the railway track for line grades of one to six (line grade one is the worst line and six is the best line) from America Railway Standard is used as input excitation, which has

$$S(\omega) = \frac{kA_v\omega_c^2}{(\omega^2 + \omega_c^2)\omega^2}, \tag{19}$$

TABLE 1

Coefficients for A_v and ω_c

Line grade	A_v(cm^2 rad/m)	ω_c(rad/m)
1	1·2107	0·8245
2	1·0181	0·8245
3	0·6816	0·8245
4	0·5376	0·8245
5	0·2095	0·8245
6	0·0339	0·8245

where A_v and ω_c are coefficients associated with line grade, as shown in Table 1, and k is a constant, normally 0·25.

4. NUMERICAL ALGORITHMS

An iterative scheme was used to analyze the dynamic response of the bridge–vehicle system by Yang and Fonder [19]. In their studies, the whole system was divided into two subsystems at the interface of the bridge and vehicles, and these two subsystems were solved separately. In a similar way, we will divide the vehicle and track coupling system into two parts, lower and upper structures, and solve them independently with the iterative scheme. Coupling the vehicle system and railway track can be realized through interaction forces between the wheels and the rail. The track vertical profile irregularity will be considered in calculating the interaction forces with the conventional Hertz formula. The advantages for analyzing the vehicle and track coupling system with the iterative scheme are: (i) we can easily solve the non-linear problem resulting from calculating interaction forces with the conventional Hertz formula shown in equation (26) and (ii) we can avoid the unsymmetrical dynamic equation for the whole coupling system.

4.1. NEWMARK INTEGRATION METHOD

In analyzing the dynamic responses of the lower structure or the upper structure, the following dynamic equation need be solved by a numerical method:

$$[M]\{\ddot{a}\} + [C]\{\dot{a}\} + [K]\{a\} = \{Q\}. \tag{20}$$

The Newmark integration method is one of the effective numerical methods, which is widely used in engineering practice. If solution ${}^t\{a\},{}^t\{\dot{a}\},{}^t\{\ddot{a}\}$ of equation (20) at time step (t) is known, solution at time step ($t + \Delta t$) can be obtained by equation (21):

$$([K] + a_1[M] + a_2[C])^{t+\Delta t}\{a\} = {}^{t+\Delta t}\{Q\} + [M](a_1{}^t\{a\} + a_3{}^t\{\dot{a}\} + a_4{}^t\{\ddot{a}\}) + [C](a_2{}^t\{a\} + a_5{}^t\{\dot{a}\} + a_6{}^t\{\ddot{a}\}), \tag{21}$$

$${}^{t+\Delta t}\{\dot{a}\} = a_2({}^{t+\Delta t}\{a\} - {}^t\{a\}) - a_5{}^t\{\dot{a}\} - a_6{}^t\{\ddot{a}\}, \tag{22}$$

$${}^{t+\Delta t}\{\ddot{a}\} = a_1({}^{t+\Delta t}\{a\} - {}^t\{a\}) - a_3{}^t\{\dot{a}\} - a_4{}^t\{\ddot{a}\}, \tag{23}$$

where $a_1 = 1/\alpha\Delta t^2$, $a_2 = \delta/\alpha\Delta t$, $a_3 = 1/\alpha\Delta t$, $a_4 = 1/2\alpha - 1$, $a_5 = \delta/\alpha - 1$, $a_6 = (\delta/2\alpha - 1)\Delta t$, α, δ are Newmark parameters. When $\alpha = 0{\cdot}25$, $\delta = 0{\cdot}5$, solution of the Newmark integration method is unconditionally stable [20].

Velocity ${}^{t+\Delta t}\{\dot{a}\}$ and acceleration ${}^{t+\Delta t}\{\ddot{a}\}$ at time step $(t + \Delta t)$ can be evaluated by equations (22,23).

4.2. ITERATION SCHEME

Assume that in time step $(t + \Delta t)$, the (k)th iteration has been done, and vectors of the displacement, velocity and acceleration at time step (t) for lower and upper structures, ${}^t\{a\}_l, {}^t\{\dot{a}\}_l, {}^t\{\ddot{a}\}_l$ and ${}^t\{a\}_u, {}^t\{\dot{a}\}_u, {}^t\{\ddot{a}\}_u$, are obtained. Now let us consider the $(k + 1)$th iteration.

(1) *Initial computation*: In the first time step and first iteration, interaction force vector ${}^0\{F\}$ should be assumed. The relative displacement between wheel and rail can be calculated by the conventional Hertz formula

$$y_i = GF_i^{2/3}, \tag{24}$$

where y_i and F_i are the relative displacement and interaction force between the ith wheel of the vehicle and the contacted rail, $G = 4{\cdot}57R^{-0{\cdot}149} \times 10^{-8}\ \mathrm{m/N^{2/3}}$ when the wheel tread is conic in shape and $G = 3{\cdot}86R^{-0{\cdot}115} \times 10^{-8}\ \mathrm{m/N^{2/3}}$ for the wheel of worn tread and R is the wheel radius.If v_{xi}, the initial displacement of the rail at contact point with the ith wheel of the vehicle, is assumed as zero, the initial absolute displacement of the ith wheel v_{wi} can be calculated by

$$v_{wi} = y_i + v_{xi}, \tag{25}$$

where both v_{xi} and v_{wi} are defined as positive in the upward direction.

(2) In the $(k + 1)$th iteration of the time step $(t + \Delta t)$, dynamic equations for lower and upper structures will be solved by stagger scheme.

Stage 1: In light of v_{wi} and v_{xi}, compute the interaction force vector ${}^{t+\Delta t}_{k+1}\{F\}_l$ as follows:

$$F_i = \begin{cases} G^{-2/3}(|v_{wi} - (v_{xi} + \eta_i)|)^{2/3}, & v_{wi} - (v_{xi} + \eta_i) < 0, \\ 0, & v_{wi} - (v_{xi} + \eta_i) > 0, \end{cases} \tag{26}$$

where F_i is the component of the interaction force vector ${}^{t+\Delta t}_{k+1}\{F\}_l$, which is the force between the ith wheel and the contacted rail, and η_i is random irregularity of the track vertical profile at the ith wheel.

Applying ${}^{t+\Delta t}_{k+1}\{F\}_l$ to the lower structure as external forces, solution of the track ${}^{t+\Delta t}_{k+1}\{a\}_l$ can be obtained by solving dynamic equation (21). Then, velocity ${}^{t+\Delta t}_{k+1}\{\dot{a}\}_l$ and acceleration ${}^{t+\Delta t}_{k+1}\{\ddot{a}\}_l$ at the $(k + 1)$th iteration of the time step $(t + \Delta t)$ can be evaluated by equations (22,23).

Stage 2: Check convergence of the solution. Compute

$$\{\Delta a\}_l^k = {}^{t+\Delta t}_{k+1}\{a\}_l - {}^{t+\Delta t}_{k}\{a\}_l, \tag{27}$$

where ${}^{t+\Delta t}_{k+1}\{a\}_l$ and ${}^{t+\Delta t}_{k}\{a\}_l$ are displacement vectors of the lower structure at current iteration and previous iteration respectively.

Now, define

$$\frac{Norm(\{\Delta a\}_l^k)}{Norm({}^{t+\Delta t}_{k}\{a\}_l)} \leq \varepsilon, \tag{28}$$

where ε is specified tolerance.

If the convergence criterion (28) is not satisfied, go to Stage 3 and continue the computation. If it is satisfied, turn to (2) and enter the next time step.

Stage 3: Compute v_{xi} according to ${}^{t+\Delta t}_{k+1}\{a\}_l$ and calculate F_i by means of equation (26). Then ${}^{t+\Delta t}_{k+1}\{F\}_u$ can be obtained.

Stage 4: Applying ${}^{t+\Delta t}_{k+1}\{F\}_u$ to the upper structure as external forces, solution of the vehicle ${}^{t+\Delta t}_{k+1}\{a\}_u$ can be obtained by solving dynamic equation (21). Then, velocity ${}^{t+\Delta t}_{k+1}\{\dot{a}\}_u$ and acceleration ${}^{t+\Delta t}_{k+1}\{\ddot{a}\}_u$ at the $(k+1)$th iteration of the time step $(t+\Delta t)$ can be evaluated by substituting ${}^{t+\Delta t}_{k+1}\{a\}_u$ to equations (22,23).

Stage 5: Compute v_{wi} according to ${}^{t+\Delta t}_{k+1}\{a\}_u$, go back to Stage 1 and continue the next iteration.

5. ANALYSES OF DYNAMIC RESPONSES OF VEHICLE AND TRACK COUPLING SYSTEM WITH RANDOM IRREGULARITY OF THE TRACK VERTICAL PROFILE

In analyses of the dynamic responses of the vehicle and track coupling system with random irregularity of the track vertical profile, TGV (French high-speed train) locomotive with three different velocities of 80, 160 and 250 km/h is considered in this paper, as shown in Figure 3. Parameters for TGV locomotive are listed in Table 2. In order to reduce the boundary effect of the rail, the total rail length for computation is 230·85 m with 405 generalized beam elements, which is more than ten times that of the vehicle. The running distance for the vehicle is 180 m. A track with two different line grades of 1 and 6 and random irregularity is studied, which is composed of 60 kg/m heavy continuously welded long rails with RC sleepers, 1760 pcs/km. The computational parameters [15, 21] are:

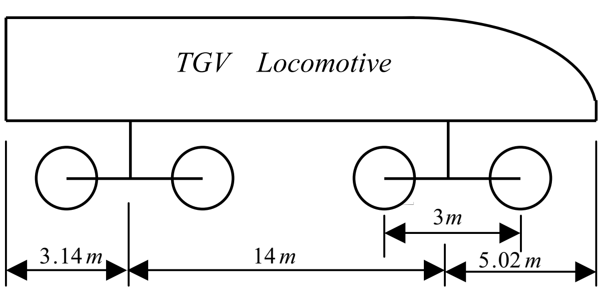

Figure 3. Layout of TGV locomotive.

TABLE 2

Parameters for TGV locomotive

Parameter	Value	Parameter	Value
Axle load	170 kN	Radius of wheel	0·458 m
Rigid wheel base	3·0 m	Mass of the car	53·5 t
Mass of bogie	3·26 t	Mass of the wheel set	2·0 t
Rigidity of unsprung mass K_{s2}	$1{\cdot}31 \times 10^3$ kN/m	Damping of unsprung mass C_{s2}	30 kN s/m
Rigidity of sprung mass K_{s1}	$3{\cdot}28 \times 10^3$ kN/m	Damping of sprung mass C_{s1}	90 kN s/m

Rail cross-section area: $A = 0{\cdot}7708 \times 10^{-2}\,\text{m}^2$, moment of inertia: $I = 0{\cdot}3203 \times 10^{-4}\,\text{m}^4$,

Modules of elasticity: $E = 2{\cdot}1 \times 10^8\,\text{kN/m}^2$, density of rail: $\rho = 7{\cdot}83 \times 10^3\,\text{kg/m}^3$,

Elastic coefficients of the support: $K_{x1} = K_{y1} = 6 \times 10^4\,\text{kN/m}$, $K_{y2} = 1{\cdot}5 \times 10^4\,\text{kN/m}$,

Damping coefficients of the support: $C_{x1} = C_{y1} = 4{\cdot}6 \times 10\,\text{kN s/m}$, $C_{y2} = 9\,\text{kN s/m}$,

Mass of the RC sleeper: $m_p = 250\,\text{kg}$, thickness of the ballast $H = 35\,\text{cm}$.

The lower and upper limit frequencies in equation (16), ω_l and ω_u, are $2\pi\,(0{\cdot}02-2)\,\text{rad/m}$ which correspond to the irregularity of the track with unevenness wavelength 0·5–50 m and N takes 2500.

In order to comprehensively understand vibration characteristics of the coupling system, analyses are performed in time and frequency domains respectively.

Results of the computations are shown in Figures 4–15. Each figure consists of four sub figures (a), (b), (c) and (d), where (a) is dynamic response in time domain and (b), c) and (d) stand for computational results in frequency domain with Cartesian, semi-log and log–log co-ordinate systems respectively. From these figures, the following is clear.

(1) The frequency distributions of the vertical interaction forces between the wheel and the rail are mainly in low-frequency area and some are in medium-frequency scope, which is due to the irregularity of the track vertical profile, as shown in Figures 4, 7, 10 and 13. For the case of line grade one and a train speed of 80 km/h, the distribution of this medium frequency is 10–40 Hz, whereas the harmonic impulses in a domain of high frequency can be seen clearly in higher grade lines as shown in Figures 7, 10 and 13, which result from excitations when wheels cross the ties periodically.

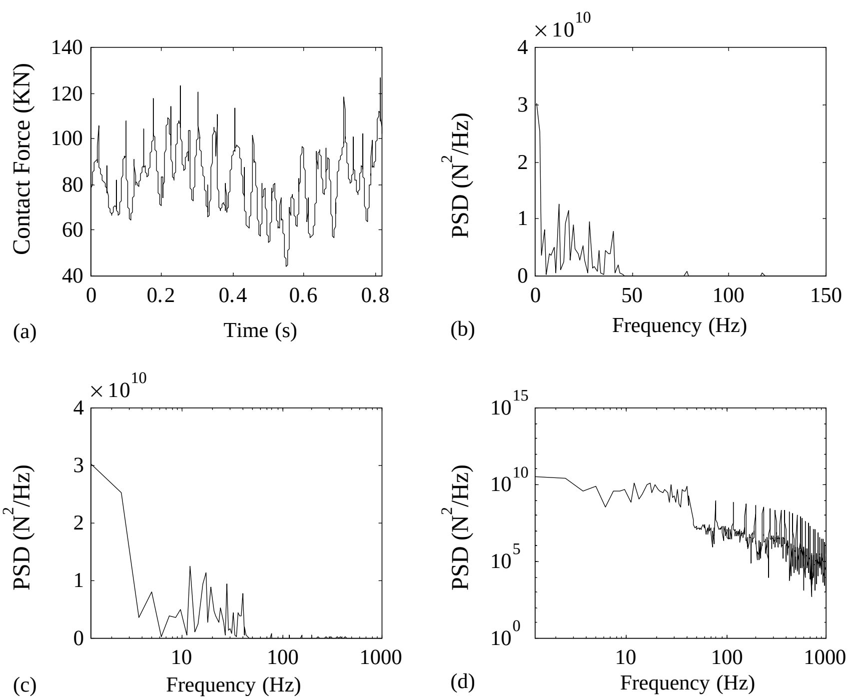

Figure 4. Interaction force between wheel and rail for line grade one and train speed of $V = 80\,\text{km/h}$.

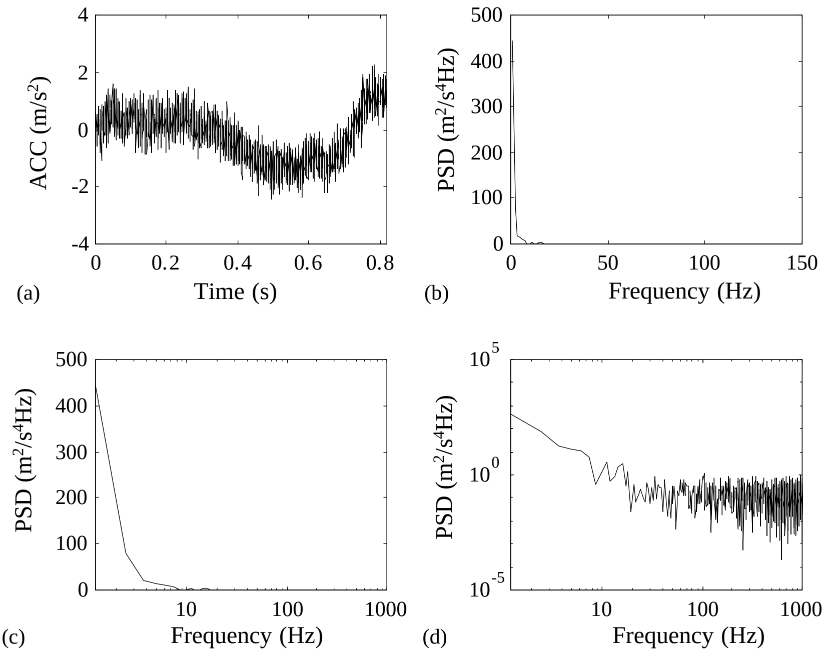

Figure 5. Acceleration of vehicle for line grade one and train speed $V = 80\,\mathrm{km/h}$.

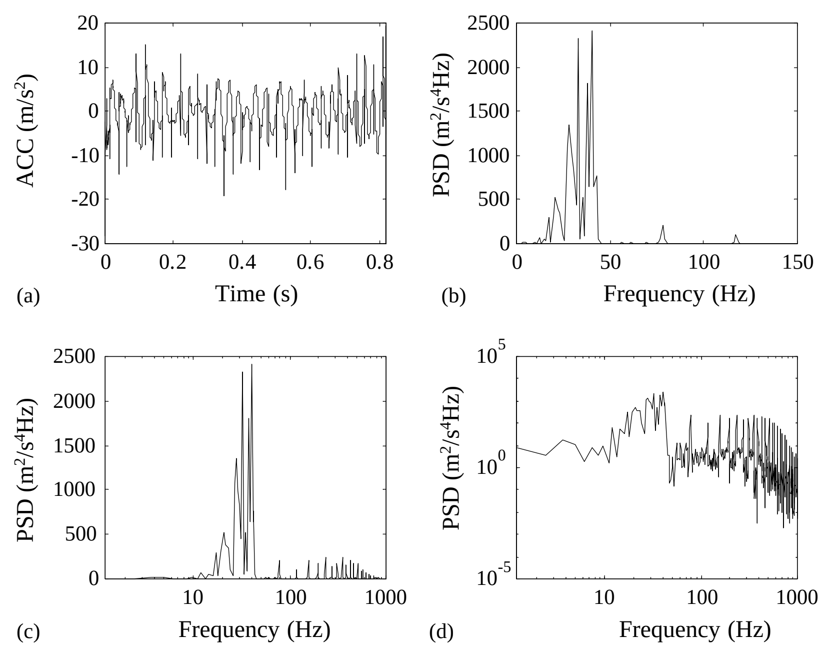

Figure 6. Acceleration of rail for line grade one and train speed $V = 80\,\mathrm{km/h}$.

(2) When the train travels at a speed of 80 km/h, the vertical acceleration of the vehicle is centralized principally in the vicinity of frequency 1 Hz, as shown in Figures 5 and 8. With increase of the train speed, vibration amplitudes of the vehicle excited by the random irregularity of the track change a little, but the frequencies shift outside up to

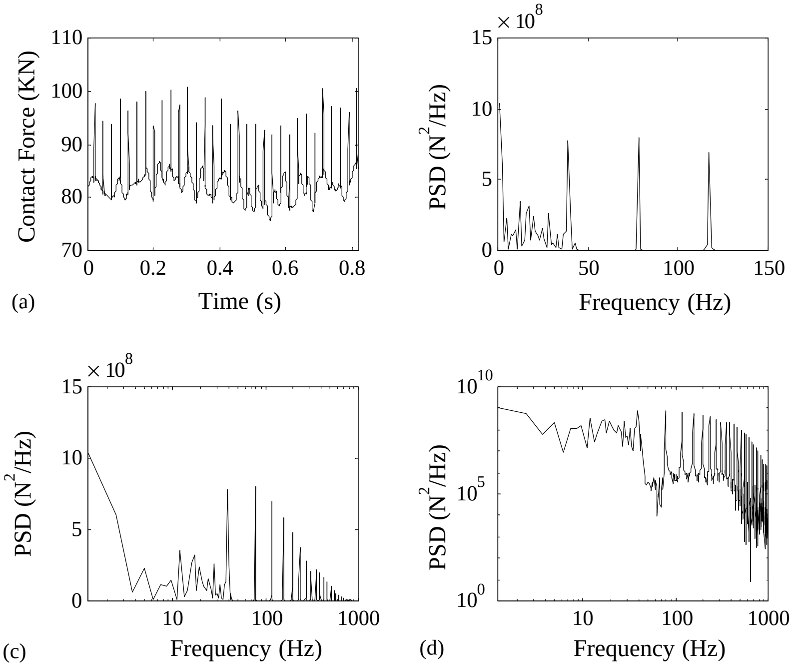

Figure 7. Interaction force between wheel and rail for line grade six and train speed $V = 80\,\mathrm{km/h}$.

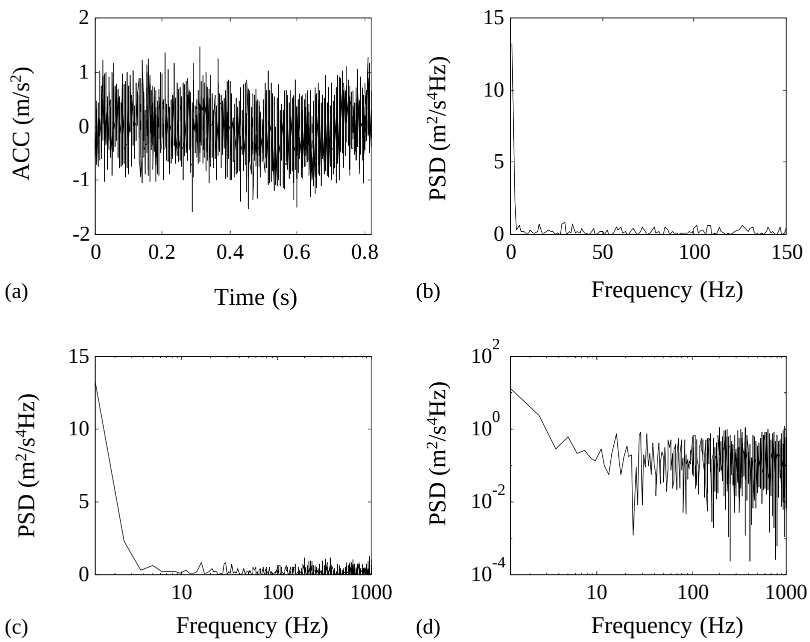

Figure 8. Acceleration of vehicle for line grade six and train speed $V = 80\,\mathrm{km/h}$.

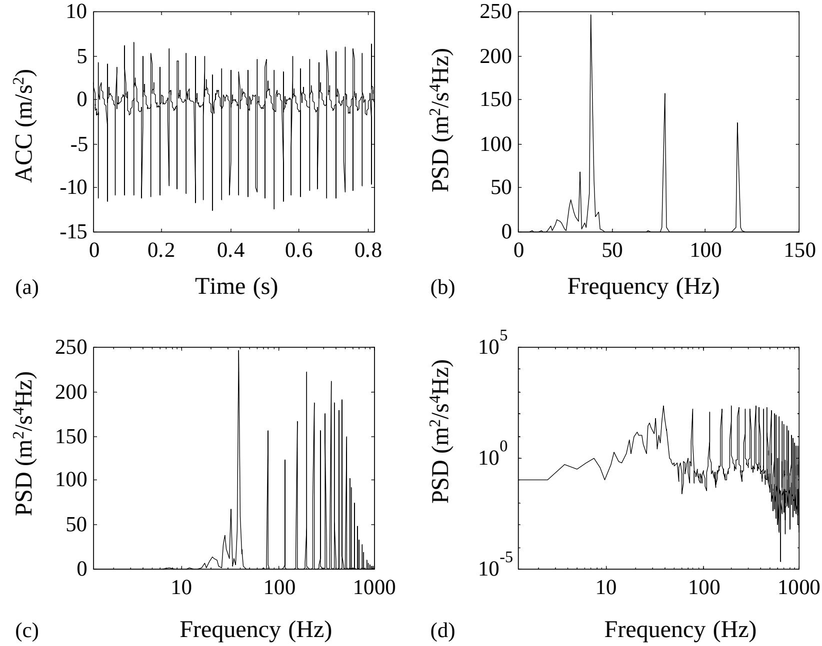

Figure 9. Acceleration of rail for line grade six and train speed $V = 80\,\mathrm{km/h}$.

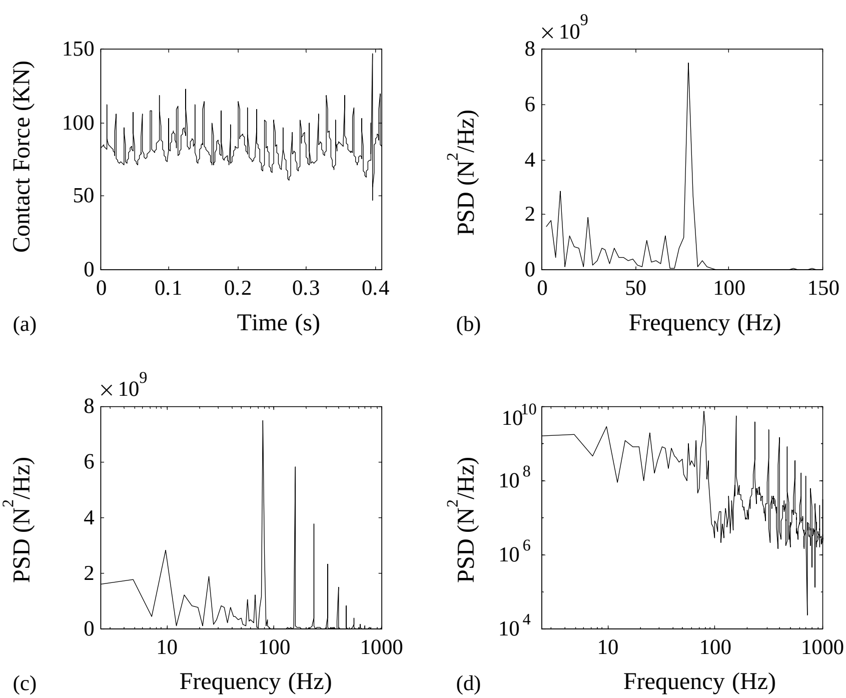

Figure 10. Interaction force between wheel and rail for line grade six and train speed $V = 160\,\mathrm{km/h}$.

domains of 5–8 Hz which are sensitive to the human body, shown in Figures 11 and 14. Therefore, the service quality of the train will be decreased in a high-speed railway.

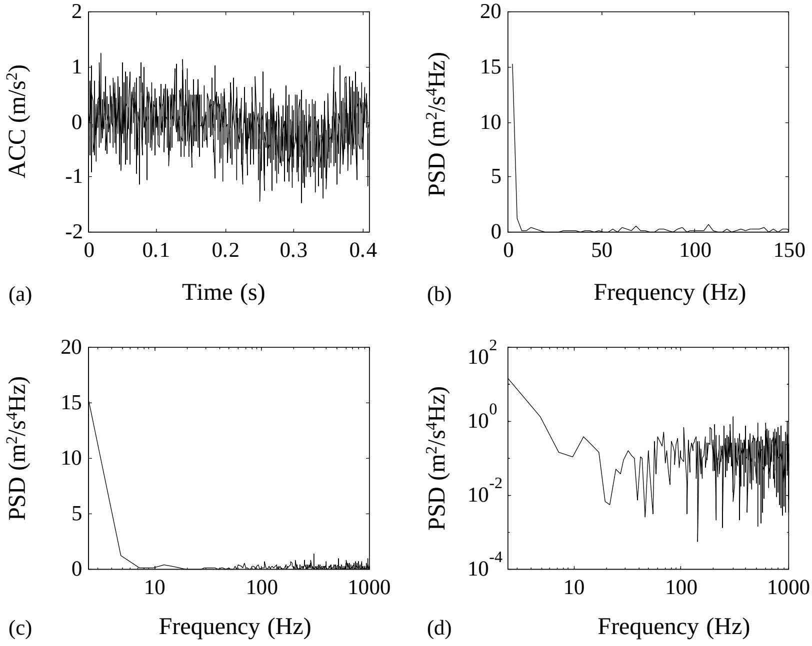

Figure 11. Acceleration of vehicle for line grade six and train speed $V = 160\,\text{km/h}$.

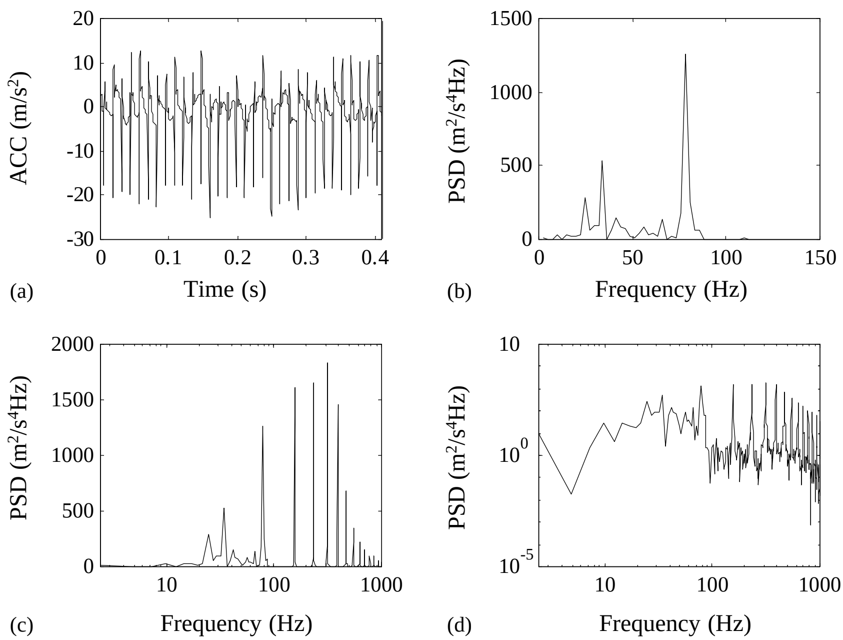

Figure 12. Acceleration of rail for line grade six and train speed $V = 160\,\text{km/h}$.

(3) Figures 6, 9, 12 and 15 show that the distribution of the vertical acceleration of the rail is in higher frequency domains and in some cases the maximum frequency can be up to 1000 Hz, which is especially true in high-speed lines and is one of the important sources of the rail noise.

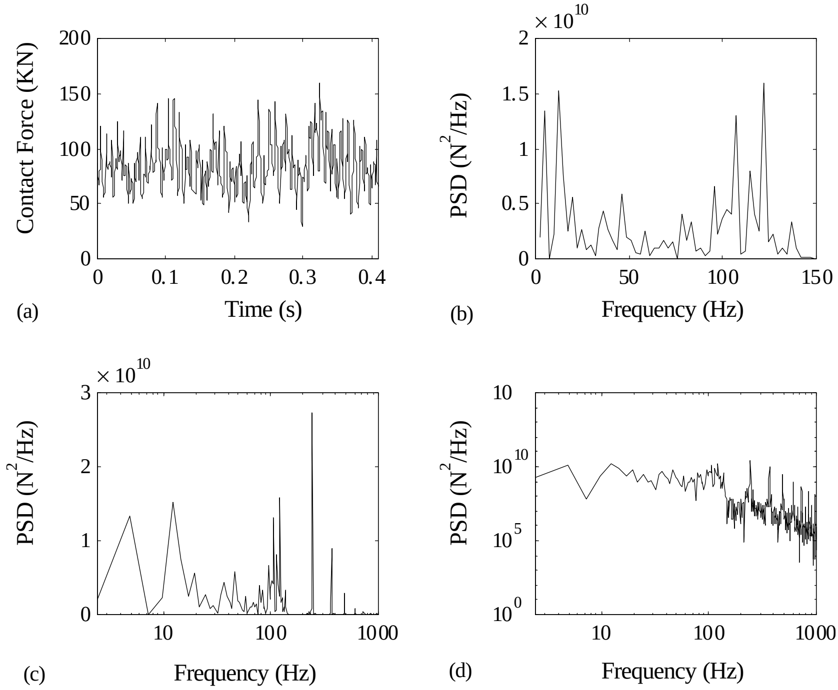

Figure 13. Interaction force between wheel and rail for line grade six and train speed $V = 250\,\text{km/h}$.

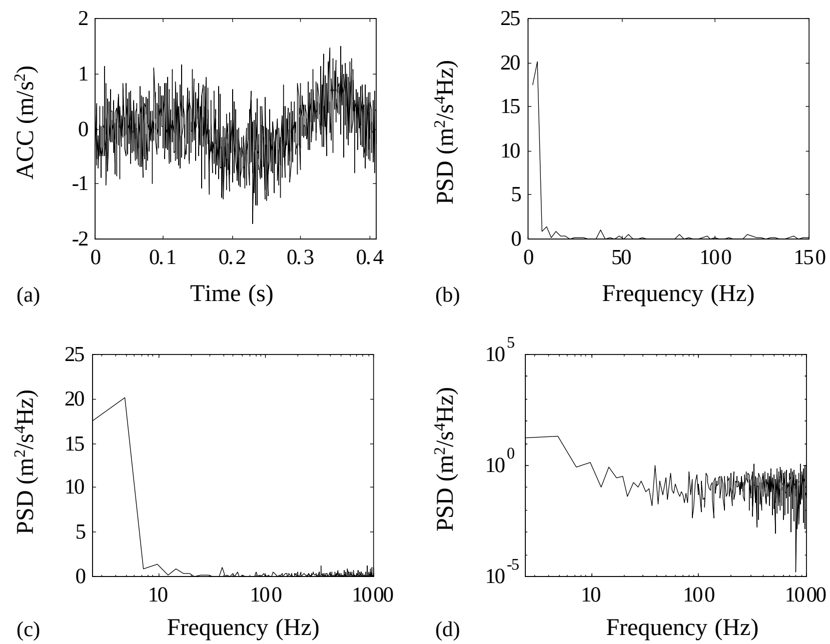

Figure 14. Acceleration of vehicle for line grade six and train speed $V = 250\,\text{km/h}$.

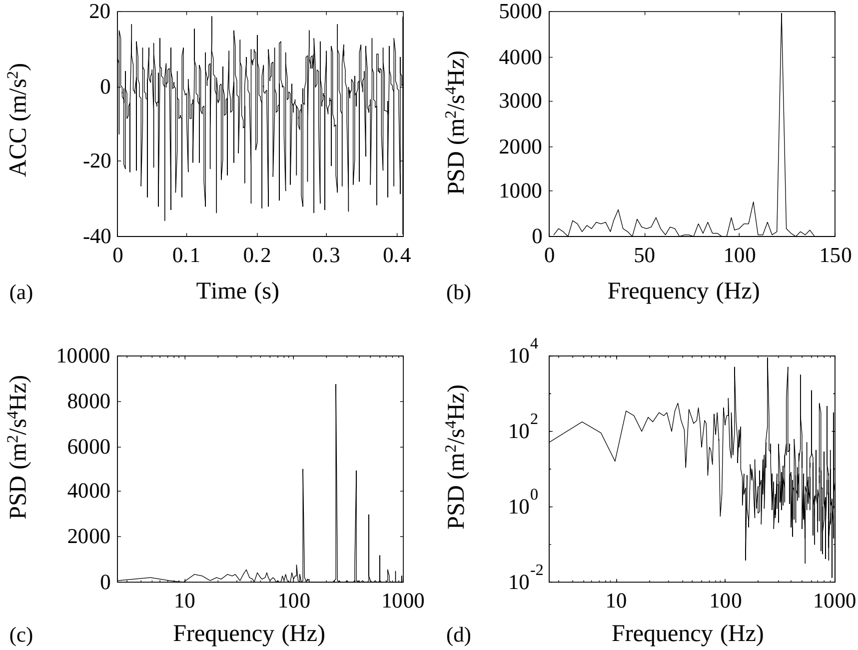

Figure 15. Acceleration of rail for line grade six and train speed $V = 250\,\text{km/h}$.

(4) The vertical interaction forces between the wheel and the rail are very sensitive both to irregularity of the track and train speeds. The maximum interaction force between the wheel and the rail is less than 100 kN for line grade six and train speed 80 km/h. However, the maximum interaction forces will be more than 120 kN for line grade one and 150 kN for train speed 250 km/h, as seen in Figures 4(a), 7(a), 10(a) and 13(a).

(5) Figures 5(a), 8(a), 11(a) and 14(a) show that the maximum vertical accelerations of the vehicle in all kinds of computational cases are less than $2\,\text{m/s}^2$ and are affected little by irregularity of the track and train speeds.

(6) Figures 6 and 9 demonstrate the acceleration amplitudes of the rail for line grades one and six with train speed 80 km/h. They are both less than $20\,\text{m/s}^2$ and are affected little by irregularity of the track with unevenness of long waves. Comparing Figure 9 with Figures 12 and 15, it is obvious that the train speed has a great effect on the acceleration of the rail, which can be up to $40\,\text{m/s}^2$ for line grade six and train speed 250 km/h.

Similar results obtained from analyses of random vibration for vehicle and track have been shown in the literature [22]. The tracks on which these analyses were carried out may consist of different track materials from those used in this paper and there are small differences between the two papers but, roughly speaking, the results of the estimations are in good accordance with those of the analyses in reference [22]. It should be pointed out that although the single TGV locomotive is investigated for simplicity of the calculation, more vehicles coupling with the track can be considered by the computational model. Even in this situation, the general features of the dynamic responses for the coupling system due to random irregularity of the track vertical profile have been obtained.

6. CONCLUSIONS

The amplitudes of vibrations, their velocities and the accelerations generated in the vehicle and rail and the interaction forces between the vehicle and the rail due to random irregularity of the track vertical profile and different line grades and train speeds have been analyzed here numerically by the vehicle and track coupling computational model. The vehicle as the upper structure in the coupling system is a whole locomotive or rolling stock with two layers of spring and damping system in which vertical and rolling motion for vehicle and bogie are involved. The lower structure in the coupling system is the railway track where rails are considered as beams with finite length resting on a double layer of continuous elastic foundation. In numerical implementation, the vehicle and track coupling system is divided into two parts, lower structure and upper structure, and solved independently with an iterative scheme. Coupling the vehicle system and railway track is realized through interaction forces between wheels and rail. The track vertical profile irregularity is considered as stationary ergodic Gaussian random processes and is simulated by trigonometry series, which is included in calculating the interaction forces with the conventional Hertz formula. The advantages for analyzing the vehicle and track coupling system with the iterative scheme are that we can easily solve the non-linear problem resulting from calculating interaction forces with the conventional Hertz formula and can thus avoid the unsymmetrical dynamic equation for the whole coupling system. Finally, as application of this coupling computational model, the vertical random vibration of the vehicle and track system under different rail line grades and train speeds is calculated and analyses of system responses are performed in time and frequency domains.

It should be pointed out that the random vibration of the vehicle and track coupling system is a very complicated problem; hence, studies on this field are still being carried out. The results and conclusions obtained in this paper are preliminary, and irregularity of track with short wavelength (less than 1 m) is not considered either.

ACKNOWLEDGMENTS

The work reported herein was supported by the KIT research fellowship program and Science Foundation of Chinese Education Ministry.

REFERENCES

1. K. Ono and M. Yamada 1989 *Journal of Sound and Vibration* **130**, 269–297. Analysis of railway track vibration.
2. R. A. Clark, P. A. Dean, J. A. Elkins and S. G. Newton 1982 *Journal of Mechanical Engineering Science* **24**, 65–76. An investigation into the dynamic effects of railway vehicles running on corrugated rails.
3. S. L. Grassie, R. W. Gregory, D. Harrison and K. L. Johnson 1982 *Journal of Mechanical Engineering Science* **24**, 77–90. The dynamic response of railway track to high frequency vertical excitation.
4. Z. Cai and G. P. Raymond 1992 *Proceedings of the 10th International Wheel Set Congress, Sydney, Australia*, 9. Theoretical model for dynamic wheel/rail and track interaction.
5. H. H. Jenkins, J. E. Stephenson, G. A. Morland and D. Lyon 1974 *Railway Engineering Journal* **3**, 2–16. The effect of track and vehicle parameters on wheel/rail vertical dynamic forces.
6. A. D. Kerr 1981 *Class Notes, University of Delaware*. Railroad Engineering.
7. M. Ishida, S. Miura and A. Kono 1998 *RTRI Report* **12**, 41–46. Track deforming characteristics and vehicle running characteristics due to the settlement of embankment behind the abutment of bridges.

8. J. C. O. Nielsen 1993 *Dissertation, Chalmers University of Technology, Goteborg, Sweden*. Train/track interaction: coupling of moving and stationary dynamic system.
9. J. Kisilowski and K. Knothe 1991 *Advanced Railway Vehicle System Dynamics*. Warsaw: Wydawnictwa Naukowo-Techniczne.
10. W. M. Zhai and X. Sun 1994 *Vehicle System Dynamics* **23** (Suppl.), 603–615. A detailed model for investigating vertical interactions between railway vehicle and track.
11. X. Y. Lei 1997 *Journal of the Chinese Railway Society* **19**, 1. Dynamic response of high speed train on ballast.
12. M. Ishida, S. Miura and A. Kono 1997 *RTRI Report* **11**, 19–26. Track dynamic model and its analytical results.
13. M. Ishida 2000 *RTRI Report* **14**, 1–6. The past and future of track dynamic models.
14. J. E. Snyder and D. N. Wormley 1977 *Journal of Dynamic Systems and Measurements Control* **99**, 23–33. Dynamic interactions between vehicle and elevated, flexible, randomly irregular guide ways.
15. X. Y. Lei 1998 *Numerical Analysis Method for Track Structure*. Beijing: Chinese Railway Publication House.
16. J. B. Roberts and P. D. Spanos 1990. *Random Vibration and Statistical Linearization*. New York: John Wiley & Sons Ltd.
17. M. Shinozuka 1971 *Journal of Accoustical Society of America* **49**, 357–368. Simulation of multivariate and multidimensional random processes.
18. IBM Application Program, System 360 Subroutine Package (360-CM-03X) Programmer's Manual H20-0205.
19. F. Yang and G. A. Fonder 1996 *Journal of earthquake engineering and structural dynamics* **25**, 195–215. An iterative solution method for dynamic response of bridge–vehicles systems.
20. O. C. Zienkiewicz 1977 *The Finite Element Method*. New York: McGraw-Hill Inc.
21. X. Y. Lei 1999 *Journal of the Eastern Asia Society for Transportation Studies*, **2**, 29–37. Research on parameters of mechanical models for track structures of high speed railway.
22. Chen Guo 2000 *Ph.D. Thesis, South West Jiaotong University*. Analysis of random vibration for vehicle and track coupling system.